Charge Division measurements with CDC prototype for GlueX

Biplab Dey, Yves Van Haarlem and Curtis A. Meyer
Carnegie Mellon University

1 Introduction

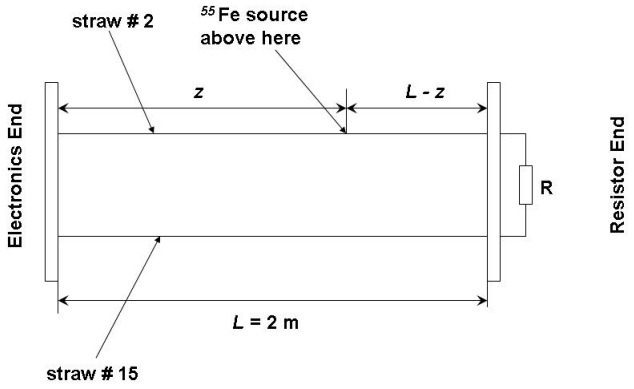

Figure 1: Setup for Charge Division measurement with a 2 m long CDC prototype.

We present results from an initial Charge Division study with a 2 m long Central Drift Chamber (CDC) prototype at Carnegie Mellon University for the GlueX experiment in Hall D, Jefferson Laboratory. Details about the construction of this prototype can be found in [1]. Our basic aim here is to determine the z position along the CDC wire closest to the passage of a charged track. This information is then to be used for further tracking purposes.

The setup is sketched in Figure 1 where we have coupled two (spatially) adjacent straw-tube wires with a resistor R. A well-collimated ^{55}Fe radiation source emitting 5.9 keV X-rays is placed immediately above straw #2. For the present setup, both straw wires were held at +1800 V. As a track passes through/around straw-tube #2 at position z it ionizes the gas inside the straw-tube, creating electron-ion pairs. The electrons subsequently drift towards the straw wire causing an accumulation of charge at the same z position. Any charge q thus created has two pathways to flow out − it can flow out through the "electronics end" (see Figure 1) of straw 2, *or*, it can flow out through the "electronics end" of straw #15 after traversing through the external resistance R ($\sim 50\ \Omega$). The total resistance that the charge will have to flow through, for a given z position, in these two scenarios are given by

$$R_2(z) = \frac{z}{L} r \tag{1}$$

$$R_{15}(z) = (\frac{L-z}{L} + 1)r + R, \tag{2}$$

where $L\,(\simeq 2\ m)$ and $r\,(\simeq 500\ \Omega)$ are the total length and the total resistance respectively, for each straw-tube wire.

This means, the total charge q created at z will be *divided* into the two channels as q_2 and q_{15}. It is easy to see that the smaller the resistance is, the more is the charge fraction flowing through a particular end. That is,

$$\frac{q_2}{q_{15}} = \frac{R_{15}}{R_2} = \frac{(2L-z)r + LR}{zr}. \tag{3}$$

The readout chain consisting of a combination of an ASIC pre-amplifier, a signal shaper board and a flash-ADC (fADC) module operating at 125 MHz (see [1] for details), placed at the "electronics end", will result in signal amplitudes for these two channels as

$$x(z) = \frac{A_2(z)}{A_{15}(z)} = \frac{(2L-z)r + LR}{zr}. \tag{4}$$

Our aim is to estimate the position z from the ratio $x(z)$.

2 Event-wise signals

Figures 2a-2c show the fADC reading versus time plots for individual events in Channels 2 and 15 (by "Channel" we refer to the fADC channel which reads out the signal from the corresponding straw tube. Thus Channel # is meant to be synonymous with straw tube #) at three different z positions. Some of the features are immediately obvious. The larger z is (closer to the "resistor end"), the less different are the two amplitudes. At the very downstream ("resistor") end, if the resistance R is small enough, the amplitudes should be nearly equal. Figure 2c shows this to be the case.

The other feature in these plots is the distinctive "tail" noticeable in both channels. This is more prominent in Channel 15, especially at low z values where the signal in this channel is mostly noise dominated (see Figure 2a). We think this is due to capacitive effects from reflection at the readout ends.

Also, initially we were triggering the fADC's by splitting the signal in Channel 2 and *externally* feeding it to the trigger. The splitter gain was seen to be causing differences in the signal shapes between Channel 2 and Channel 15. For all measurements presented here, we used an *internal* trigger programmed in the fADC. Aside the "tail", the signal shapes in Channel 2 and Channel 15 are then seen to follow each other quite well.

3 Amplitude ratios

Figure 3 shows the distribution of $\frac{A_2}{A_{15}}$ for $z = 176\ cm$. Here A_i is defined as the global maximum amplitude in the i^{th} channel, subtracted by the corresponding pedestal value. At lower values of z, where the signal in Channel 15 decreases correspondingly, it is sometimes difficult to pick out a global maximum because of the noise. For our purposes here, we know that Channel 2 will always have a bigger signal. We thus choose a common "time window" for both channels as the shortest time interval containing the maximum crest in Channel 2.

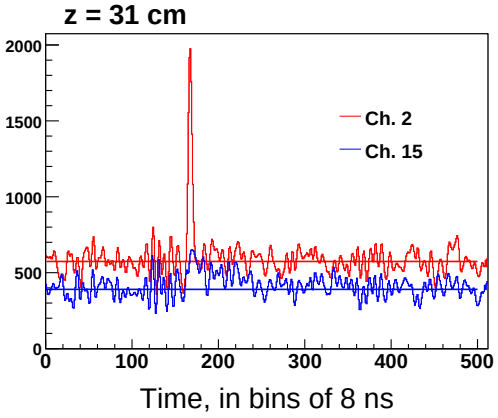

(a)

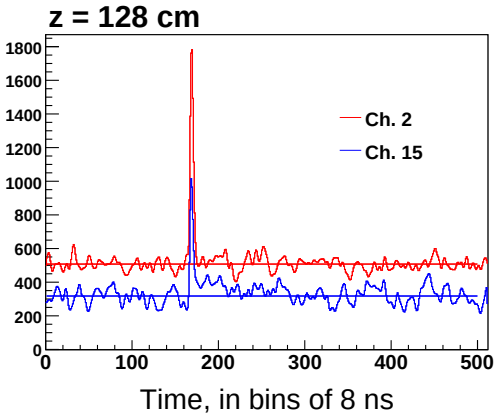

(b)

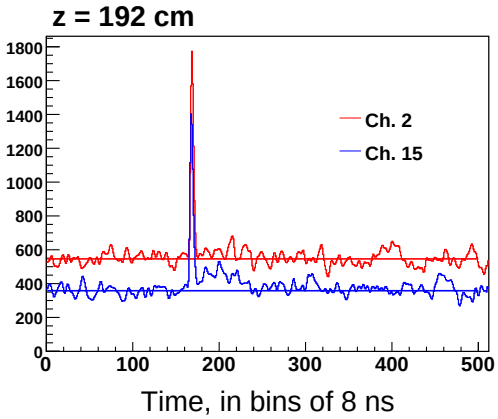

(c)

Figure 2: fADC output versus time for individual events at three different z positions. The horizontal lines show the pedestal values for each channel calculated from the first 100 time samples.

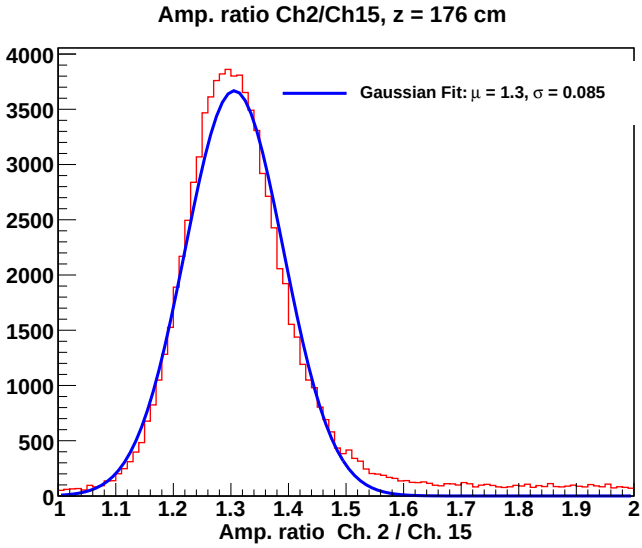

Figure 3: Amplitude ratio distribution and extraction of ratio mean and error characterestics for a particular z.

The ratio distribution is then fit to a Gaussian and the fit characterestics (mean μ and width σ) are ascribed to the ratio measurement. In this way, we map out the ratios and estimated errors over an extended range of z. This is shown in Figure 4.

We plot the ratio both versus z and $1/z$, because, from Equation 4, the amplitude ratio should be linear with $1/z$. The linear behavior is approximately followed above $z \sim 100\ cm$. Below this value, that is close to the "electronics end", the output in Channel 15 is dominated by noise. A_{15} is thus more often than not, over-estimated, because of the small signal being buried under noise with both the signal and the noise having almost overlapping periodicities.

4 Error Estimation

Figure 4 shows the mean ratios μ (in red) within a "band" of $\pm\sigma$ (in blue). This provides a way to estimate the error Δz for a particular value of $A_2(z)/A_{15}(z)$. Figure 5 shows a close-up at the "resistor end" z where things are more or less linear. Note that this is also the region where we expect most of the tracks to pass through in the final version.

For a given $A_2(z)/A_{15}(z)$, one can see that the horizontal span of the error band is $\Delta z \sim \pm 10\ cm$. Given that the total length of the wires for charge division is 4 m, one nominally expects (from earlier Charge Division measuremts in the Crystal Barrel experiment) a $\sim 1\%$, or $\sim \pm 4\ cm$ error. With the present prototype, our estimated errors are roughly twice this value. However, we know that the present prototype has issues with noise. In the final version, with better noise insulation, the errors are likely to go down.

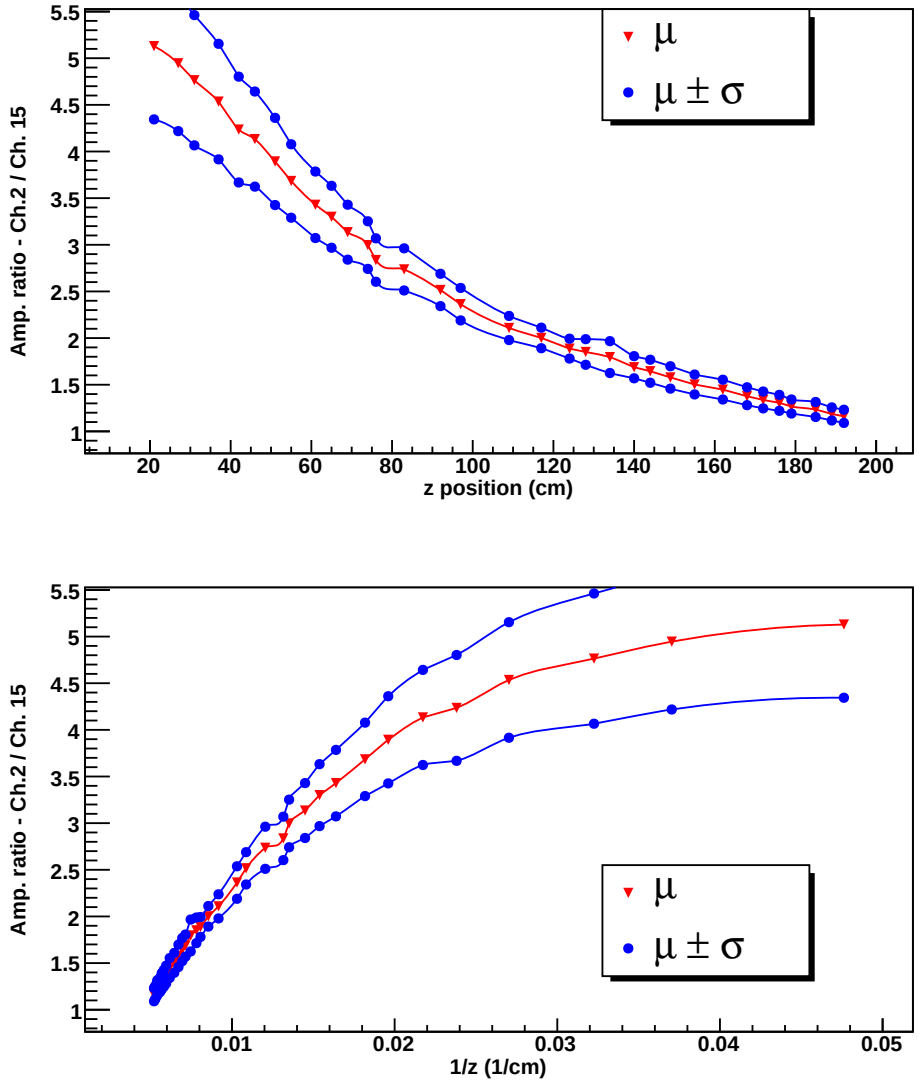

Figure 4: Charge Division: mapping between $A_2(z)/A_{15}(z)$ and z. See text for details.

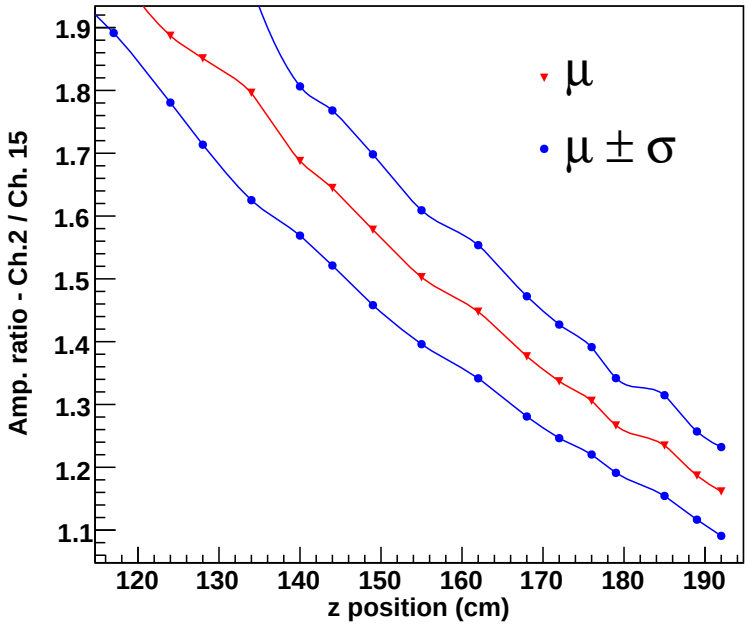

Figure 5: Close-up of the signal ratio vs. z plot at the downstream end. Estimated z resolution is roughly ± 10 cm.

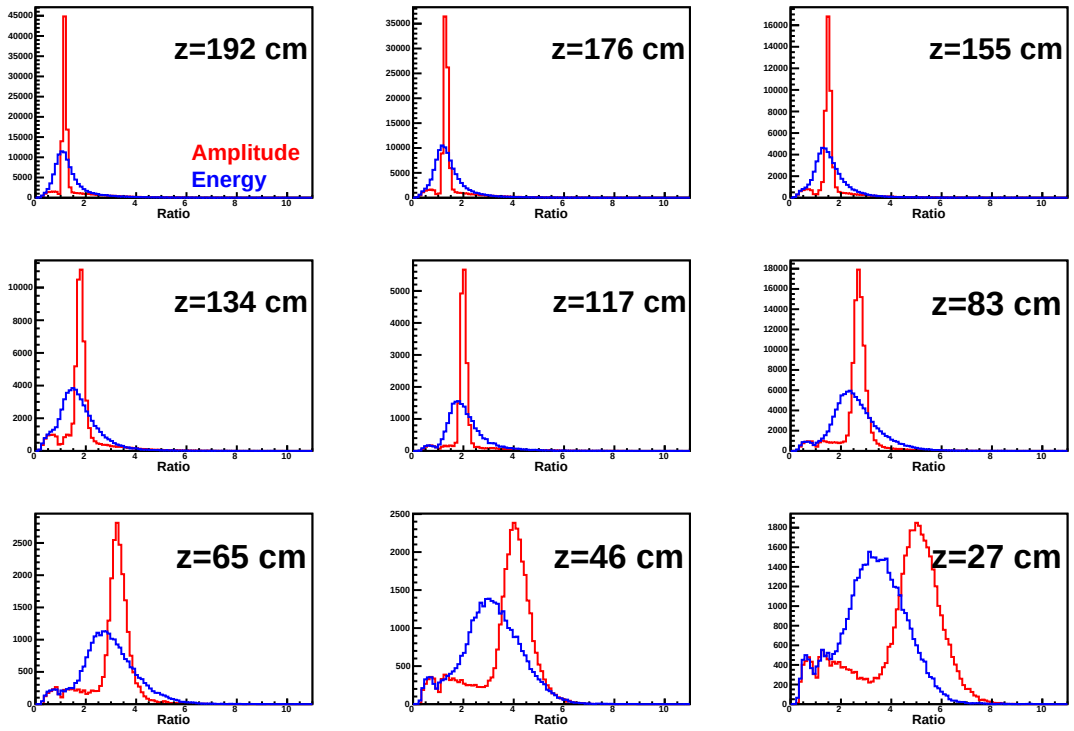

Figure 6: Signal strength ratios between Channel 2 and Channel 15 – Amplitude ratios (in red) and Energy ratios (in blue), for different z positions. The latter is always wider and appears to peak at a lower value than the former.

5 Energy ratios

Instead of amplitude ratios, one can also define the signal strength ratios to be the integrated signal (or equivalently, energy) ratios between two channels. Assuming one is using a sufficiently wide integration range, this should lead to better noise cancellations over a localised reading of amplitude ratios. However, for the present purposes, the noise period ($T \sim 60\ ns$) is roughly equal to the signal duration and thus the calculated energy is very sensitive to the integration range.

We first extract a rough estimate of the noise period from the first 100 time samples. Within statistical fluctuations, this is, as noted earlier, roughly around 60 ns. We take the position of the first minimum after the maximum amplitude as the end time t_2. The start time t_1 is then taken as $t_2 - nT$, where n is an integer (we took $n = 6$ and 8). For low z's, the signal in Channel 15 is sometimes inseparable from noise. For this reason, we opted to test run a second version with a common integration time window as obtained from Channel 2. All four versions gave similar results.

The results are shown in Figure 6 for different z values for $n = 8$ and a common integration time window. The integration ratio distributions are always wider, signifying larger estimated errors and also appears to peak at a lower value than the amplitude ratios (especially for lower z positions). Thus, under the present circumstances, we do not seem to be gaining anything by going to energy integrations from amplitudes. The main limitation is noise, augmented by the fact that the noise seems to have a time period roughly the same as the signal duration.

6 Summary

We have performed an initial set of Charge Division measurements on a 2 m long CDC prototype with satisfactory results. The main limitation in the measurements is noise, especially if the z position is close to the readout "electronics end". Our estimated Δz is around ± 10 cm. We have also compared results from using amplitude ratios and energy ratios as a measure of the relative signal strength between two channels. We found that the amplitude ratio works best under the present circumstances. This could however change with better noise insulation. A newer prototype with much better overall engineering and noise control has already been manufactured at Carnegie Mellon (however, for portability purposes it was made to be much smaller, which is not ideal for Charge Division measurements). As our analysis demonstrates here, with a well-calibrated and noise-insulated chamber, Charge Division measurement can be a very useful supplement towards z position tracking.

References

[1] Y. Van Haarlem and C. A. Meyer, **The CDC ASIC for GlueX**, GlueX-doc-1079, (2008)